Rock and Soil Mechanics

Volume 44 | Issue 8 Article 6

12-6-2023

A calculation method for deformation of diaphragm wall of narrow deep foundation pit in soft soil considering spatio-temporal effect

Kun-yong ZHANG
Key Laboratory of Ministry of Education for Geomechanics and Embankment Engineering, Hohai University, Nanjing, Jiangsu 210024, China; Geotechnical Research Institute, Hohai University, Nanjing, Jiangsu 210024, China

Meng ZHANG
Geotechnical Research Institute, Hohai University, Nanjing, Jiangsu 210024, China

Bin SUN
Jiangsu Zhongshe Group Co. Ltd., Wuxi, Jiangsu 214072, China

Fu-dong LI
China Communications Construction Co., Ltd-Second Highway Bureau Fourth Engineering Co., Ltd., Luoyang, Henan 471000, China

See next page for additional authors

A calculation method for deformation of diaphragm wall of narrow deep foundation pit in soft soil considering spatio-temporal effect

Abstract

To accurately evaluate the safety of foundation pit construction in soft soil area and its impact on the surroundings, the time and space influencing factors during excavation cannot be ignored. In this paper, based on the excavation of a deep foundation pit in the soft soil area of the Yangtze River floodplain, a 3D finite element model was established considering the combination of bottom-up and top-down constructions, and the calculated values of horizontal displacement of the diaphragm wall were compared with the measured values to verify the reliability of the finite element calculation. Based on theoretical analysis, numerical calculation and measured data, the influence coefficient of corner effect and equivalent horizontal resistance coefficient were used to measure the influence of spatio-temporal effect on the deformation of supporting wall, and the calculation method of the diaphragm wall deformation considering spatio-temporal effect was proposed. The necessity of the spatio-temporal effect and the rationality of the proposed method in the design of foundation pit in soft soil area were verified by engineering examples. The results can provide beneficial reference for the calculation of deep foundation pit deformation in soft soil area.

Keywords

foundation pit excavation, numerical simulation; spatio-temporal effect, retaining structure deformation calculation

Authors

Kun-yong ZHANG, Meng ZHANG, Bin SUN, Fu-dong LI, and Yong-zhou JIAN

Rock and Soil Mechanics 2023 44(8): 2389−2399 ISSN 1000−7598
https://doi.org/10.16285/j.rsm.2022.6114 http://rocksoilmech.researchcommons.org/journal

A calculation method for deformation of diaphragm wall of narrow deep foundation pit in soft soil considering spatio-temporal effect

ZHANG Kun-yong[1, 2], ZHANG Meng[2], SUN Bin[3], LI Fu-dong[4], JIAN Yong-zhou[4]

1. Key Laboratory of Ministry of Education for Geomechanics and Embankment Engineering, Hohai University, Nanjing, Jiangsu 210024, China
2. Geotechnical Research Institute, Hohai University, Nanjing, Jiangsu 210024, China; 3. Jiangsu Zhongshe Group Co. Ltd., Wuxi, Jiangsu 214072, China
4. China Communications Construction Co., Ltd-Second Highway Bureau Fourth Engineering Co., Ltd., Luoyang, Henan 471000, China

Abstract: To accurately evaluate the safety of foundation pit construction in soft soil area and its impact on the surroundings, the time and space influencing factors during excavation cannot be ignored. In this paper, based on the excavation of a deep foundation pit in the soft soil area of the Yangtze River floodplain, a 3D finite element model was established considering the combination of bottom-up and top-down constructions, and the calculated values of horizontal displacement of the diaphragm wall were compared with the measured values to verify the reliability of the finite element calculation. Based on theoretical analysis, numerical calculation and measured data, the influence coefficient of corner effect and equivalent horizontal resistance coefficient were used to measure the influence of spatio-temporal effect on the deformation of supporting wall, and the calculation method of the diaphragm wall deformation considering spatio-temporal effect was proposed. The necessity of the spatio-temporal effect and the rationality of the proposed method in the design of foundation pit in soft soil area were verified by engineering examples. The results can provide beneficial reference for the calculation of deep foundation pit deformation in soft soil area.

Keywords: foundation pit excavation; numerical simulation; spatio-temporal effect; retaining structure deformation calculation

1 Introduction

A large-scale development of underground space has been carried out in China since the beginning of 21st century, and a great many of subway station excavations has shown a trend of "deep, large and long"[1−2]. The ultra-deep large foundation pit of the subway station on which this study is based is in the soft soils of the Yangtze River floodplain, where the soil has a high void ratio and compressibility, low shear strength, and is prone to large deformation during excavation[3]. To ensure the safety and stability of the foundation pit and reduce the negative impact on the surroundings, the retaining structure deformation needs to be strictly controlled in the process of the excavation[4−5]. Time and space are the two most influential factors on excavation engineering in soft soils[6], so the spatio-temporal effects on the deformation of the retaining structure during excavation needs to be considered to analyze and predict the stress and deformation of the foundation pit more accurately and ensure the construction safety [7−8].

A deep foundation pit is a three-dimensional structure with length, width, and depth[9−10], and the stress and deformation of the retaining structure is obviously affected by the spatio-temporal effect. The spatio-temporal effect refers to the space factors such as three-dimensional size, shape, and segmentation of the foundation pit and its retaining system, as well as the time factors such as excavation time, unsupported time, and the elapsed time between excavation stages, which make the stress and deformation of the soil elements and the retaining structure at different locations distinct. Liu et al.[11−12] was the first to propose the method for predicting the deformation of foundation pits with considering the spatio-temporal effect, controlling the deformation through the construction method of "layering, partitioning, balancing, symmetry, and time limiting". Liu et al.[13] developed a practical method for calculating the internal force and deformation of the retaining structure in soft soil areas on the base of the finite bar element method, accounting for the spatio-temporal effect. Ying et al.[14] studied the temporal effect during excavation by finite element method coupled with Biot's consolidation theory and suggested combining the soil permeability coefficient, the excavation rate, and the elapsed time between excavation stages when studying the effect of soil consolidation. Harahap et al. [15] investigated the time-dependent deformation of diaphragm wall for a typical excavation in soft clay and believed that the deformation of the diaphragm wall was affected greatly by the soil creep and less by the consolidation. Li et al.[16] found that the range of spatial effect was mainly affected by the excavation depth and the internal friction angle of soils after studying the calculation model of the horizontal displacements of the retaining structure of a long and narrow deep foundation pit considering the spatial effect.

The temporal effect is affected by the excavation stress path and excavation time, and the spatial effect is related to the three-dimensional size of a foundation pit and excavation conditions. In the finite element analysis, a constitutive model adapted to the stress path of foundation pit excavation should be selected and the actual working conditions should be simulated[17],

Received: 18 July 2022 Accepted: 14 March 14 2023
This work was supported by the National Natural Science Foundation of China (41530637).
First author: ZHANG Kun-yong, male, born in 1975, PhD, Professor, mainly engaged in teaching and research on the basic soil properties, soil–structure interaction, and numerical analysis of geotechnical engineering. E-mail: ky_zhang@hhu.edu.cn

so as to accurately reflect the influence of space-time effect. However, the retaining design method recommended in the codes is often simplified as a two-dimensional plane problem for calculation and analysis, which cannot reflect the impact of spatiotemporal effects on the stress and deformation of the retaining structure during the excavation process of the foundation pit. At present, the design of retaining structure for deep foundation pits is shifting from control of strength to that of deformation, so it is necessary to fully consider the spatio-temporal effect during excavation [18–19]. Additionally, it is also necessary to optimize the design and calculation methods recommended in the Codes, proposing an improved method for predicting the deformation of retaining structures of deep foundation pits in soft soil areas.

In this study, the coefficients of corner effect and equivalent horizontal resistance were employed to characterize the spatio-temporal effect on the deformation of retaining structure, and the calculation method of deformation of diaphragm wall considering spatio-temporal effect was proposed, based on theoretical analysis, numerical calculations and measured data attained from an actual deep large foundation pit. The results can enrich the theory of spatio-temporal effect and provide reference for similar projects.

2 Project overview

2.1 Project description

Figure 1 shows the location plan of the foundation pit at Mochou Lake Station of Nanjing Metro Line 7. The total length of the pit is 160.0 m, with a width of 22.4 m and a depth of 33.5 m deep in the standard section, and the shafts at the north and south ends are of 26.8 m depth and 35.0 m width. This is a station of underground four-storey island platform. The combination of bottom-up and top-down construction methods was adopted for the main structure, i.e., the underground first and second storeys were constructed via bottom-up method while the underground third and fourth storeys were constructed using top-down method.

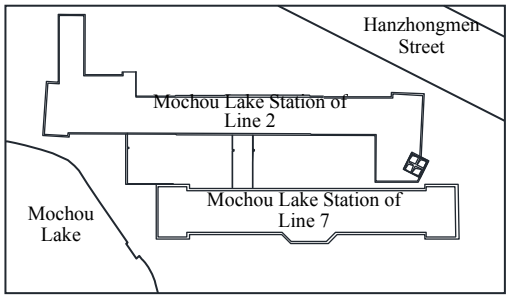

Fig. 1 Location plan

2.2 Engineering geological and hydrogeological conditions

The station is built in the soft soil layer of the Yangtze River floodplain, with a high groundwater level. The soils mainly consist of silty clay, muddy silty clay, silt, and silty sand in an interbedded form, with soil parameters shown in Table 1. The groundwater at the site mainly occurs in three categories: pore phreatic water in the upper loose layer (near −1 m), pore confined water, and fissure water in the weathered zone of bedrock.

Table 1 Soil parameters

No.	Soil layer	Layer thickness /m	Unit weight /(kN • m^{-3})	K_0	v	Saturated unit weight /(kN • m^{-3})	e	c /kPa	φ /(°)	E_s /MPa
1	Plain fill	2.5	18.7	0.60	0.38	21.2	0.94	11.74	16.33	3.78
2	Muddy silty clay	11.0	17.6	0.70	0.43	19.7	1.14	12.51	25.08	3.39
3	Silty clay, muddy silty clay	3.0	17.9	0.55	0.35	19.8	1.07	9.65	30.78	4.46
4	Silty sand	9.5	18.8	0.38	0.28	20.1	0.86	4.91	29.79	8.59
5	Silty clay with silty sand	3.0	18.2	0.50	0.33	19.8	1.01	9.83	34.86	5.05
6	Silty sand	4.0	18.9	0.35	0.28	20.2	0.86	4.66	30.23	8.31
7	Silty clay with silty sand	13.0	18.1	0.50	0.33	19.8	1.01	9.83	34.86	5.05
8	Silty-fine sand	10.0	19.0	0.32	0.24	20.8	0.76	0.32	32.27	9.95
9	Weathered rock	—	23.3	0.25	0.42	22.4	0.63	25.00	48.00	45.00

2.3 Design of retaining structure

A diaphragm wall and bracings were adopted as the retaining system. The diaphragm wall was 1.2 m thick and 64.0 m deep, divided by a 0.8 m thick and 64.0 m deep blocking wall into two sections: the large mileage section was 102.0 m long, and the small mileage section was 58.0 m long.

A total of six bracing layers were set up along the depth direction of the diaphragm wall, with the 1st, 5th, and 6th concrete bracing layers and the 2nd, 3rd, and 4th ϕ609 steel bracing layers. The 1st layer was composed of 0.7 m×0.8 m concrete bracing, and the average horizontal spacing between bracings was 6.0 m; the average spacing between the steel bracings in the 2nd, 3rd, and 4th layers was 3 m; the concrete bracings in the 5th and 6th layers were 1 m×1 m with an average spacing of 4.5 m. The prestresses of the 2nd, 3rd, and 4th steel bracing layers for the large and small mileage sections were 700, 1,000, and 1,200 kN and 600, 800, and 1,000 kN, respectively. The cross-section view of the foundation pit is shown in Fig. 2.

2.4 Construction and monitoring

Following the principle of layering, segmenting, and blocking, the excavation was processed in eight segments along the long side of the foundation pit, as shown in Fig. 3.

The main structure was constructed by the bottom-up and top-down methods combined. The vertical

retaining structure was completed first, and then layered excavation was processed from top to bottom, with the first to fourth bracing layer set one by one; after excavating to the baseplate of the underground second storey, the floor slabs were constructed from bottom to top and the bracings were removed; finally, the top plate was backfilled to restore the ground, so that the bottom-up construction of the underground first and second storeys was completed. From the baseplate of the second underground storey, excavation from top to bottom in storeys was processed and then the bracings layers and floor slabs were constructed, one storey excavation for one storey construction, until the completion of the main structure; finally, the bracings were removed, thereby the top-down construction of the underground third and fourth storeys was completed.

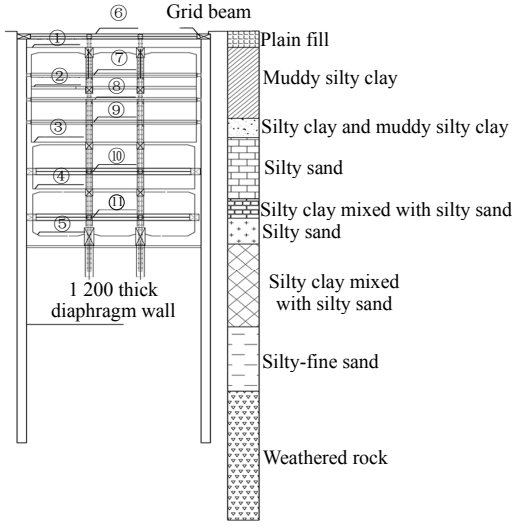

①—Top plate of underground 1st storey; ②—Baseplate of underground 1st storey
③—Baseplate of underground 2nd storey; ④—Baseplate of underground 3rd storey
⑤—Baseplate of underground 4th storey; ⑥—1st concrete strut layer
⑦—2nd steel strut layer; ⑧—3rd steel strut layer; ⑨—4th steel strut layer
⑩—5th concrete strut layer; ⑪—6th concrete strut layer

Fig. 2 Cross-section of foundation pit

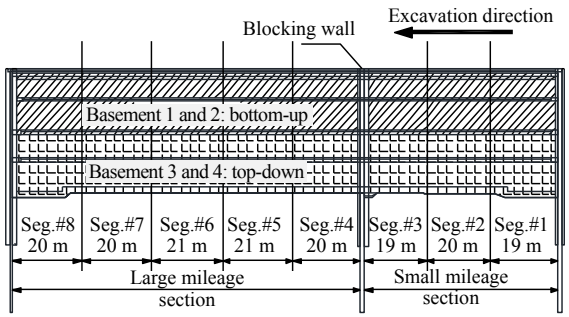

Fig. 3 Illustration of segmented bracing excavation

An inclinometer buried in the diaphragm wall was used to monitor deep horizontal displacement. The monitoring points were ZQT1–ZQT20, distributed as shown in Fig.4. In the subsequent analysis, the data from ZQT9 when the construction of the bracing layer or floor slab was finished were selected as the monitoring value for the mid-span of large mileage.

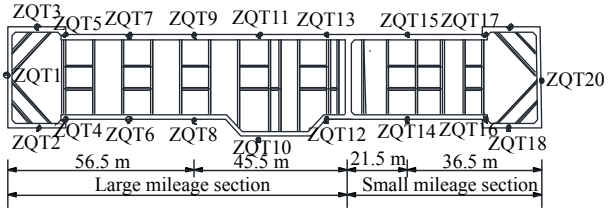

Fig. 4 Distribution of the monitoring points for the horizontal displacement of the diaphragm wall

3 Three-dimensional finite element analysis of retaining structure considering construction process

The finite element software Midas GTS was used to establish a three-dimensional model of the deep foundation pit, realistically simulating the excavation process, analyzing the deformation of the diaphragm wall, and comparing with the measured values to verify the rationality of the finite element calculation. According to the existing studies, the factors affecting the temporal effect was unified as time step in the finite element simulation, which was a simulation of the construction process without considering the influence of soil creep separately.

3.1 Constitutive model and selection of parameters

The traditional constitutive model is established on the base of the laboratory axial loading test, which makes it difficult to simulate the soil stress–strain law under the condition of excavation stress path. Based on the Cam–clay model, the Ohta–Sekiguchi model rotates the hardening axis to change the yield surface in the *p*-*q* plane from the original *p*-axis isotropic hardening to anisotropic hardening along the K_0 axis, which reduces the elastic zone under the unloading stress path and can partly reflect the effects of K_0 consolidation and excavation stress paths.

Soil layers with different properties have different impacts on the excavation stability, and the soft soil is more prone to large deformation than sand, so it is necessary to adopt different constitutive models for soil layers with different properties. In this study, the Ohta–Sekiguchi model was employed for the soft soil, the modified Mohr–Coulomb model was for sand, and the linear elasticity model was for retaining structures. The parameters were derived from the survey data and laboratory tests, with details shown in Tables 2 and 3.

Table 2 Material parameters of retaining structure

Type	Unit weight /(kN • m^{-3})	Modulus of elasticity /MPa	Poisson's ratio	Design strength /MPa
Concrete strut, diaphragm wall and floor slab (C35 concrete)	24.5	31 500	0.167	11
Steel strut(ϕ609)	78.5	206 000	0.300	30

Table 3 Parameters of the Ohta–Sekiguchi constitutive model

Soil layer	λ	κ	M
Muddy silty clay	0.110	0.014	1.073
Silty clay, muddy silty clay	0.117	0.016	1.233
Silty clay with silty sand	0.132	0.020	1.410

3.2 Finite element modelling

For the analysis domain of the three-dimensional finite element model, the length extending outward on both sides of the foundation pit is twice the excavation depth of the foundation pit, the length extending downwards at the bottom is twice the excavation depth of the foundation pit. Based on the realities and engineering experience, the model was set as the size of 360 m×22 6m×100 m, with a total of 226,674 elements and 346,692 nodes. The initial groundwater level was 1 m from the surface, and a total water head of 99 m was set in the seepage boundary to simulate the initial groundwater level. During the excavation process, dewatering was conducted for four times, each time lowering to 1 m below the subsequent excavation surface, which was realized by setting a constant water head boundary at 1 m below the excavation surface. The consolidation module was selected to set the excavation time, the unsupported time, and the elapsed time for each working condition. Boundary constraints were set for the model: displacement constraints in the *X, Y, Z* directions were applied at the bottom of the soil boundary, displacement constraints in the *X, Y* directions were applied at four sides, and the upper boundary was free. An operation of deactivated and activated elements was used to simulate the earth excavation and the construction of retaining structure. The finite element model and simulation of segmented bracing excavation are shown in Figs. 5 and 6.

The segmented bracing excavation followed the order of first corners and then middle, first small mileage section and then large mileage section. At the same depth, the first and second underground storeys were constructed bottom-up firstly in segments 1 and 2, then in segments 3, 7 and 8, and finally in segments 4, 5 and 6; the third and fourth underground storeys were constructed via top-down procedure, firstly in segments 1, 2 and 8, and then in segments 3, 4 and 7, and finally in segments 5 and 6. The construction sequence of each segment is shown in Table 4, in which the construction at the previous stage is one construction step ahead of the next one.

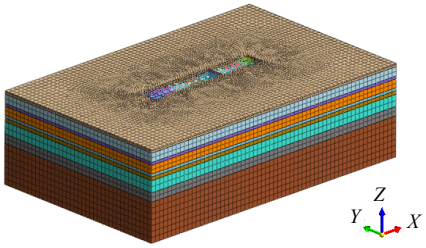

Fig. 5 Three-dimensional finite element model of foundation pit

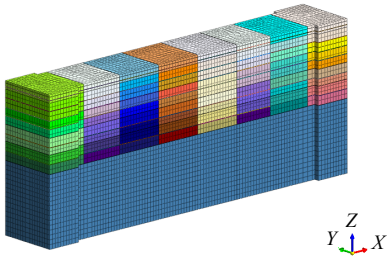

Fig. 6 Section diagram of foundation pit

3.3 Numerical analysis

Five typical construction stages in the excavation process at the mid-span of the large mileage section were selected for analysis, i.e. the excavation to the bottom of the second steel strut layer (referring to the retaining structure in Section 2.3), to the baseplate of the second underground storey, the completion of the bottom-up construction, excavation to the baseplate of the third underground storey, and to the baseplate of the fourth underground storey, with the corresponding excavation depths of 6.5, 18, 18, 25, and 33.5 m. The horizontal displacements of diaphragm wall were calculated by selecting the corresponding deformation value after earth excavation was completed with unsupported and before the construction of struts or floor slabs. The calculation results of the three-dimensional model at each stage were compared with the measured values, as shown in Fig. 7.

Table 4 Construction stages

Stage	Excavation depth /m	Details	Time step /d			
			Earth excavation	Unsupported	Constructions	Intermittent time
1	—	Retaining structure (dewatering)	—	—	—	—
2	1.0	Strut layer 1	1	1	6	7
3	6.5	Strut layer 2 (dewatering)	5	1	2	21
4	11.0	Strut layer 3	6	1	2	16
5	14.5	Strut layer 4	6	1	2	20
6	18.0	Baseplate of the second underground storey	7	3	13	14
7	18.0	Baseplate of the first underground storey (dismantling strut layers 3, 4)	—	—	14	13
8	18.0	Top plate of the first underground storey (dismantling strut layers 2, 1 in sequence; dewatering) The bottom-up construction of the underground first and second storeys was completed after the top plate was backfilled. Later, it was suspended for about 103 days because of COVID-19.	—	—	13	—
9	22.0	Strut layer 5	7	2	8	12
10	25.0	Baseplate of the third underground storey (dewatering)	6	3	13	8
11	29.0	Strut layer 6	7	2	9	14
12	33.5	Baseplate of the fourth underground storey (dismantling strut layers 5, 6 in sequence)	10	4	18	—

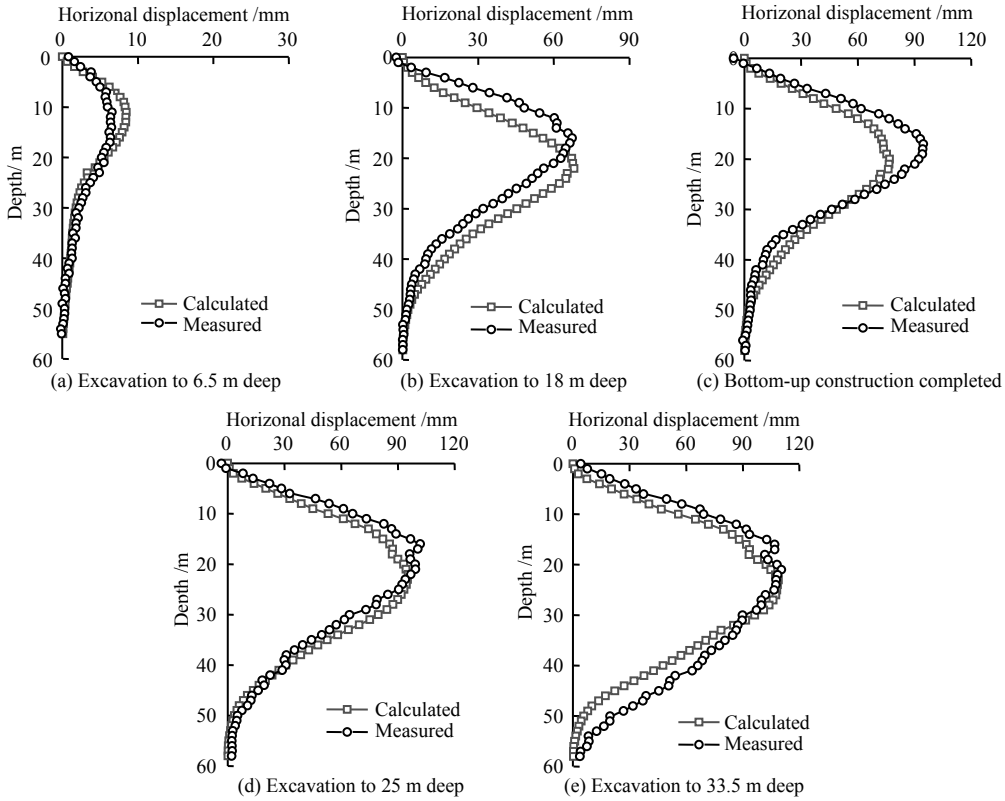

Fig. 7 Comparison of horizontal displacements of diaphragm wall

The horizontal displacement curves in Fig.7 shows a bulging shape with small values at two ends and big values at middle in general. With the increase of excavation depth, the maximum horizontal displacement and the corresponding depth are increasing, and the spatio-temporal effect becomes more and more significant. One of the reasons for the gap between the calculated and the measured values may be that the influence of soil creep on the temporal effect was not considered in the finite element simulation. However, the calculated results are generally consistent with the measured values in terms of numerical values and distribution patterns, which verifies the reliability of the three-dimensional model and proves that the finite element calculation based on the Ohta-Sekiguchi model can well reflect the spatio-temporal effect on the retaining structure deformation during the deep foundation pit excavation. The calculation results of the numerical model can be used to derive the formula for calculating the horizontal displacement of the diaphragm wall considering the spatio-temporal effect.

4 Spatio-temporal effect on retaining structure deformation

4.1 Spatial effect on retaining structure deformation

The spatial effect is mainly affected by the aspect ratio L/B of the foundation pit and the excavation length–depth ratio L/H [20]. Along the depth direction, the deformation of the diaphragm wall is small at both ends and large in the middle; along the length direction, the lateral displacement of the diaphragm wall is usually the maximum in the middle of the long side of the pit, and gradually decreases to both ends, reaching the minimum at the corner. The overall deformation is illustrated in Fig. 8.

Wang et al. [21] defined the coefficient of the corner effect K_{ij} as

$$K_{ij}=\frac{\delta_{ij}}{\delta_j} \tag{1}$$

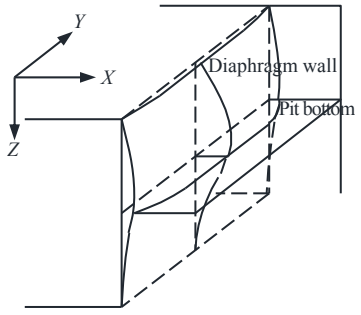

Fig. 8 Schematic diagram of retaining structure deformation

where δ_{ij} is the horizontal displacement of the point at the horizontal distance i from the pit corner and at depth j from the ground surface; δ_j is the horizontal displacement of the middle part of the retaining structure at depth j from the ground surface without the spatial effect.

To study the distribution of K_{ij} in the large mileage section, the three-dimensional model range is 56 meters from the corner to the mid span in the long side direction of the large mileage section, and to the middle of each underground storey along the depth

direction, namely, the depths of 6.0, 13.5, 22.0, and 29.0 m. The calculated horizontal displacements and K_{ij} at different depths at five typical construction stages were analyzed, as shown in Fig. 9.

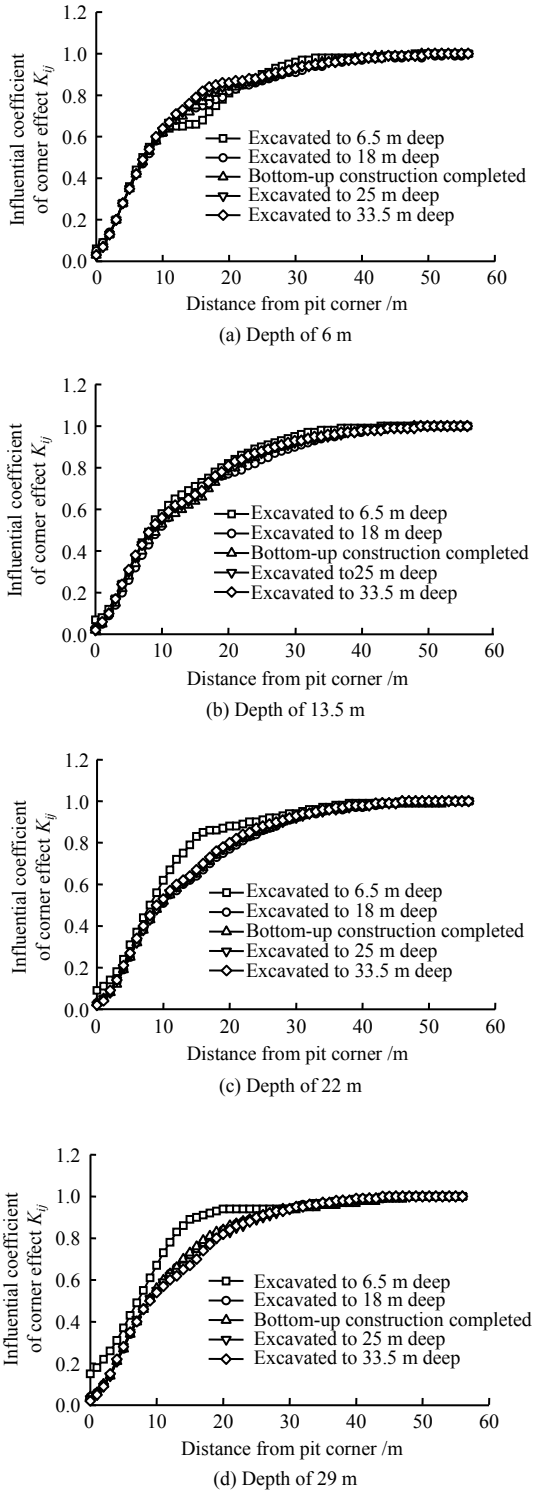

Fig. 9 Distribution of influence coefficients of corner effect at different stages

As shown in Fig.9, The deformation of the diaphragm wall at each stage is the smallest at pit corners, and gradually increases from the corners to the mid-span, approaching a constant value. Therefore, the spatial effect within a certain range of the midspan can be neglected when the aspect ratio is large. At the same depth, only the distribution of K_{ij} at the excavation depth of 6.5 m quite differs from that at other excavation depth. It can be deemed that the distribution patterns of K_{ij} below a certain excavation depth will tend to be consistent and is not affected by the construction stages and the excavation depths. The influence of L/H can hence be neglected in the study of K_{ij} after the pit is excavated to a certain depth.

Five sets of calculations were carried out for the pits with different L/B based on the three-dimensional finite element model mentioned previously, with B as 22.4 m, and L/B as 1.76, 2.56, 3.65, 4.58, and 5.39. The distribution of the horizontal displacements of the diaphragm wall at the depth of 22 m at the completion of the bottom-up construction was selected to study the effect of L/B on K_{ij}. The retaining structure deformation, K_{ij}, and its change rate K' within the half-span are shown in Figs. 10 to 12.

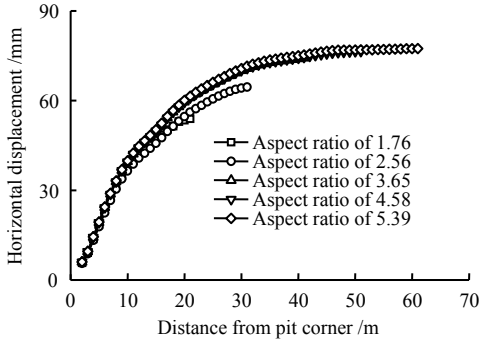

Fig. 10 Horizontal displacements of diaphragm wall

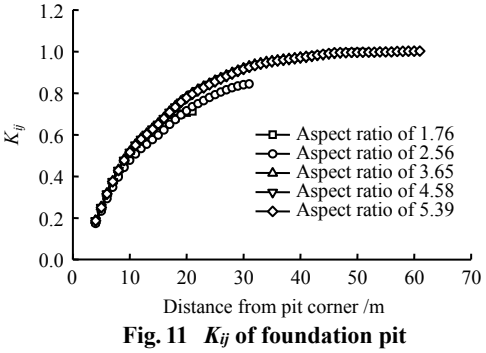

Fig. 11 K_{ij} of foundation pit

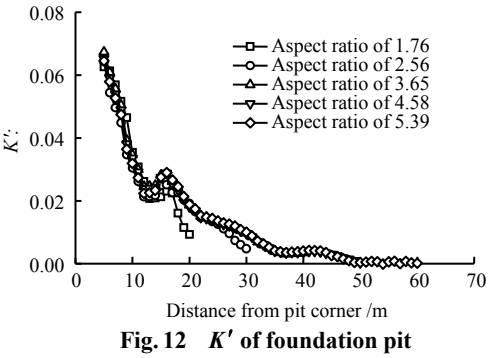

Fig. 12 K' of foundation pit

K' is distributed exponentially overall, fitted by using the function $K' = a \cdot \exp(bx + c)$, with a always

being 0.025. The relationship of b and c with L/B is identified as shown in Fig. 13.

The relationship of K' versus L/B is

$$K' = 0.025 \cdot \exp\left(\left(0.006\frac{L}{B} - 0.11\right)x - 0.07\frac{L}{B} + 1.6\right) \tag{2}$$

After K_{ij} is fitted by the function $K_{ij} = A + \frac{a}{b}\exp(bx + c)$, the relationship of the constant A to L/B is obtained as shown in Fig. 14.

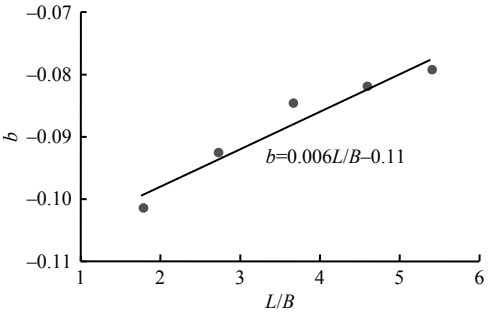

(a) Relationship of b and aspect ratio

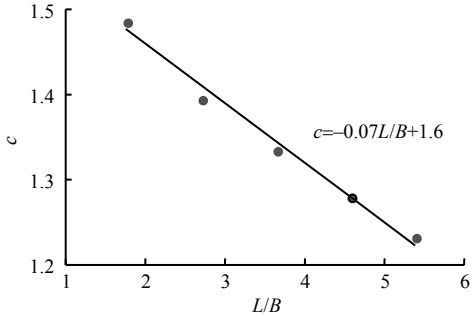

(b) Relationship of c and aspect ratio

Fig. 13 Relationship between *b*, *c* and aspect ratio

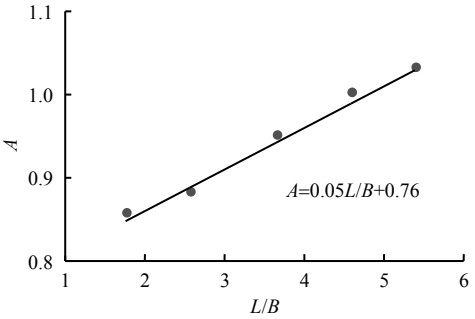

Fig. 14 Relationship of constant *A* with aspect ratio

Therefore, the relationship of K_{ij} to L/B is

$$K_{ij} = 0.76 + 0.05\frac{L}{B} + \frac{4.17}{\frac{L}{B} - 18.33} \cdot \exp\left(\left(0.006\frac{L}{B} - 0.11\right)x - 0.07\frac{L}{B} + 1.6\right) \tag{3}$$

4.2 Temporal effect on deformation of retaining structure

An equivalent horizonal resistance coefficient K_h accounting for the factors including excavation time, excavation depth, unsupported time and soil parameters, is proposed to characterize the temporal effect on the deformation of the retaining structure. With the continuous excavation, K_h tends to decrease overall, first fast and then slow. In the depth direction, K_h is unevenly distributed, large in deep soil and reduced significantly after excavation. Liu et al. [22] proposed the formula for calculating K_h of a ground without reinforcement as

$$K_h = 635\alpha_r\alpha_c\alpha_s\alpha_d \tag{4}$$

where α_r is the influential coefficient of soil rheology: $\alpha_r = \exp[(12.0 - T_j)/T_j]$, T_j is the unsupported time (h) during the foundation pit excavation.

α_c is the influential coefficient of soil strength:

$$\alpha_c = \frac{\gamma_i \tan^2\left(\frac{\pi}{4} + \frac{\varphi_i}{2}\right) + 4c_i \tan\left(\frac{\pi}{4} + \frac{\varphi_i}{2}\right)}{1.42\gamma_i + 47.6} \tag{5}$$

where γ_i is the unit weight of the soil in layer i (kN/m^3); c_i is the cohesion of the soil in layer i (kN/m^2); φ_i is the internal friction angle of the soil in layer i (°); α_s is the coefficient of spatial effect in the depth direction, $\alpha_s = \frac{8}{B_j} + 0.1$, where B_j is the area of the excavated soil along the wall (m^2); and α_d is the correction factor of depth:

$$\alpha_d = \left(1 - \frac{h_j}{h_i}\right)\left\{1 - \frac{2\gamma_i'\left[1 - \left(1 - \frac{h_j}{h_i}\right)^{0.36}\right]\tan\varphi_{cq}}{\gamma_i + 2\gamma_i'\tan\varphi_{cq}}\right\} \tag{6}$$

where φ_{cq} is the strength parameter at point h_i to be calculated; h_j is the depth of the current excavated surface (m); γ_i' is the buoyant unit weight of the soil in Layer i (kN/m^3).

The relationship of α_r with the unsupported time is shown in Fig. 15.

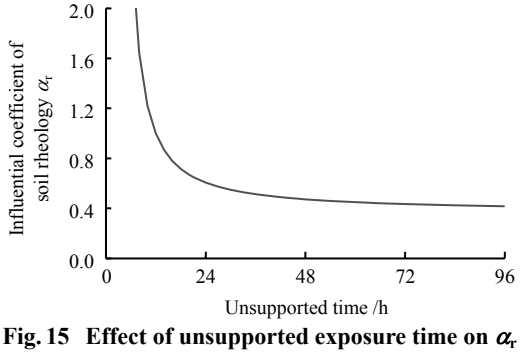

Fig. 15 Effect of unsupported exposure time on α_r

Figure 16 shows the variation of α_d at different depth with the excavation depth.

The influence of each factor on K_h is coupled mutually, so it is necessary to conduct the finite element calculations with all the factors considered to

analyze the variation of the horizontal displacement increments of the diaphragm wall during the elapsed time after the completion of a specific construction stage. The selected construction stage is shown in Table 5.

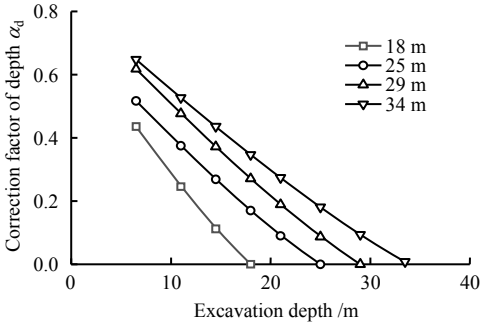

Fig. 16 Variation of depth correction coefficient α_d

Table 5 Stages selected for model analysis

Stage	Excavation depth /m	Area of the excavated soil along the wall /m²	Unsupported time /d	Construction details
1	11.0	3.0	0.5	Strut layer 3
2	14.5	3.5	1.0	Strut layer 4
3	18.0	3.5	2.0	Baseplate of the second underground storey
4	22.0	4.0	4.0	Strut layer 5
5	25.0	3.0	8.0	Baseplate of the third underground storey
6	29.0	4.0	16.0	Strut layer 6
7	33.5	4.5	32.0	Baseplate of the fourth underground store

Only the unsupported exposure time differed among the time factors of the seven selected construction stages. The horizontal displacement increments and growth rates of the diaphragm wall at depths of 25, 29, and 33.5 m are shown in Figs. 17 and 18.

The increment of deformation of the retaining structure varies exponentially–linearly, which corresponds to the variation pattern of K_h that integrates α_r and α_d. Therefore, in terms of the deformation of retaining structure, the calculated results by the K_h formula is in line with those by the finite element method, which can reflect well the temporal effect along the depth direction.

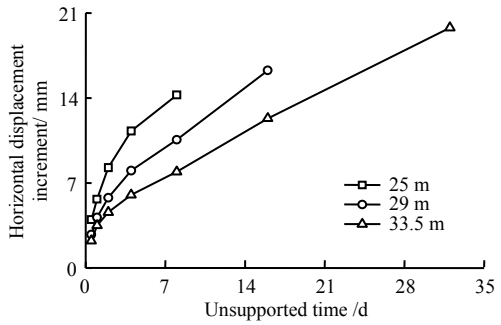

Fig. 17 Horizontal displacement increment of diaphragm wall

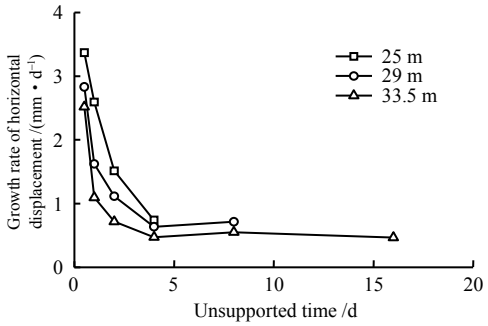

Fig. 18 Growth rate of horizontal displacement of diaphragm wall

5 Calculations of diaphragm walls deformation considering spatio-temporal effect

5.1 Calculation method

The actual deformation increment of the retaining structure in the depth direction after earth excavation includes two parts: the first deformation increment u_1 is calculated by the method of vertical beam on elastic foundation in the *Code*, without considering the spatio-temporal effect; the second deformation increment u_2 is generated because of the reduction of the horizontal resistance coefficient of the soil, with the consideration of the spatio-temporal effect. The schematic diagrams of the deformation increments are shown in Fig. 19.

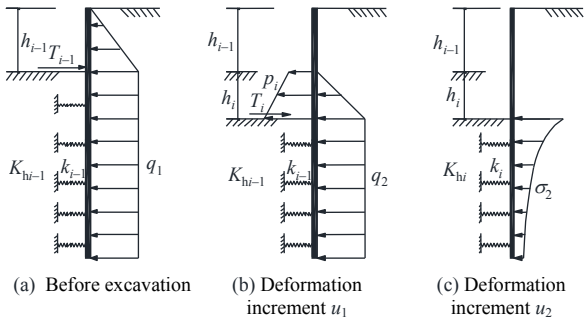

Fig. 19 Schematic diagram of calculation of retaining structure deformation increment

In the elastic foundation beam method, the soil and the retaining structure are modeled as spring elements, and the earth excavation is represented by reducing the soil springs. The reduction of the soil springs leads to changes in the overall spring horizontal stiffness, which needs to be modified. The modified horizontal stiffness of the soil spring k_i is calculated by the following formula:

$$k_i = \frac{K_{hi-1}}{K_{hi}} k_{i-1} \tag{5}$$

where k_{i-1} is the soil spring stiffness under the (i–1)-th working condition; K_{hi-1} is the equivalent horizontal resistance coefficient under the (i–1)-th working condition.

After calculating u_1 by the software for retaining structure of foundation pit, considering the spatio-temporal effects on K_h, the calculation formula of

u_2 is deduced as follows:

$$\Delta k = \left|k_i - k_{i-1}\right| = k_i\left(\frac{K_{\mathrm{h}i-1}}{K_{\mathrm{h}i}} - 1\right) \tag{6}$$

$$\sigma_2 = u_1 \Delta k = u_1 k_{i-1}\left(\frac{K_{\mathrm{h}i-1}}{K_{\mathrm{h}i}} - 1\right) \tag{7}$$

$$u_2 = \frac{\sigma_2}{k_i} = u_1\left(1 - \frac{K_{\mathrm{h}i}}{K_{\mathrm{h}i-1}}\right) \tag{8}$$

where σ_2 is the force corresponding to the u_2; k_i is the modified soil spring stiffness under the *i*-th working condition.

$$u = u_1 + u_2 = u_1\left(2 - \frac{K_{\mathrm{h}i}}{K_{\mathrm{h}i-1}}\right) \tag{9}$$

$$U_n = \sum_{i=1}^{n} u_{\mathrm{i}} = \sum_{i=1}^{n} u_{i1}\left(2 - \frac{K_{\mathrm{h}i}}{K_{\mathrm{h}i-1}}\right) \tag{10}$$

By introducing the coefficient of corner effect K_{ij}, the calculation formula of retaining structure deformation considering spatio-temporal effect is attained:

$$U_{n_{ij}} = K_{ij} U_n = K_{ij} \sum_{a=1}^{n} u_{\mathrm{a}1}\left(2 - \frac{K_{\mathrm{h}a}}{K_{\mathrm{h}a-1}}\right) \tag{11}$$

where $U_{n_{ij}}$ is the horizontal displacement of the retaining structure at the distance *i* from the pit corner and the depth *j* from the ground surface under the *n*th working condition; u_{a1} is the deformation increment under condition *a* without considering the spatio-temporal effect; $K_{\mathrm{h}a}$ is the equivalent horizontal resistance coefficient under condition *a*; and $K_{\mathrm{h}a-1}$ is the equivalent horizontal resistance coefficient under condition $a-1$.

5.2 Case study

The proposed method was used to calculate and analyze the deformation of the diaphragm wall in the excavation process of the foundation pit of Mochou Lake station. Since the spatio-temporal effects can be neglected at the mid-span of the pit with a large aspect ratio, a two-dimensional analysis was conducted using FRWS software. The mid-span of the large mileage section was taken for calculation, and u_1 was solved by the method in the *Code*. The cross-section of the bracing excavation is shown in Fig. 20, and the details at construction stages are shown in Table 6.

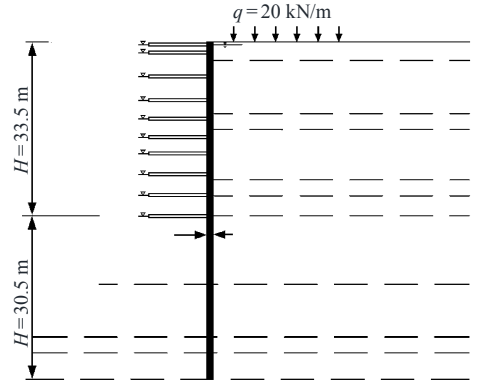

Fig. 20 Cross-section of the foundation pit excavation

Table 6 Foundation pit excavation stage

Working condition	Construction details	Unsupported time /h	Area excavated along the wall /m²
1	Excavated to −1 m deep, Strut layer 1 constructed	24	1.0
2	Excavated to −6.5 m deep, Strut layer 2 constructed	12	5.5
3	Excavated to −11 m deep, Strut layer 3 constructed	12	4.5
4	Excavated to −14.5 m deep, Strut layer 4 constructed	12	3.5
5	Excavated to −18 m, the baseplate of the second underground storey constructed	48	3.5
6	Strut layers 3 and 4 are dismantled in sequence, the baseplate of the first underground storey constructed at −9 m	—	—
7	Strut layers 2 and 1 dismantled in sequence, the top plate of the first underground storey constructed at −2 m	—	—
8	Excavated to −22 m deep, Strut layer 5 constructed	24	4.0
9	Excavated to −25 m, the baseplate of the third underground storey constructed, Strut layer 5 dismantled	48	3.0
10	Excavated to −29 m deep, Strut layer 6 constructed	24	4.0
11	Excavated to −33.5 m, the baseplate of the fourth underground storey constructed, Strut layer 6 dismantled	48	4.5

The horizontal displacement u_1 without considering spatio-temporal effect at five typical construction stages are compared with the measured values, as shown in Fig. 21.

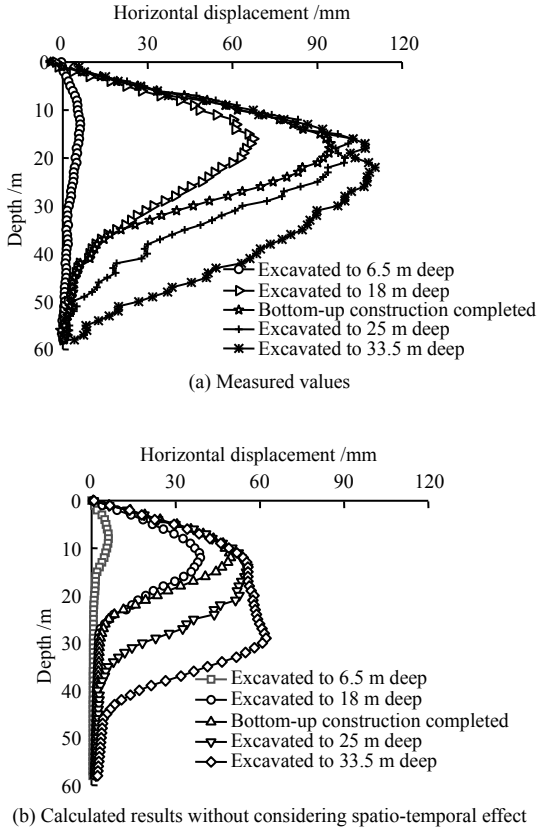

(a) Measured values

(b) Calculated results without considering spatio-temporal effect

Fig. 21 Horizontal displacements of diaphragm wall at different stages

It is found that the calculation results without considering spatio-temporal effect are significantly smaller than the measured values, the deformation distribution also differs and becomes more and more different with the increase of excavation depth. Therefore, the spatio-temporal effect on the deformation of the retaining structure should not be ignored and must be taken into account in the design of the foundation pit engineering.

To consider the spatio-temporal effects, the horizontal displacements of the diaphragm walls at the above five typical construction stages are calculated using the proposed method, and then compared with the measured values, as shown in Fig. 22.

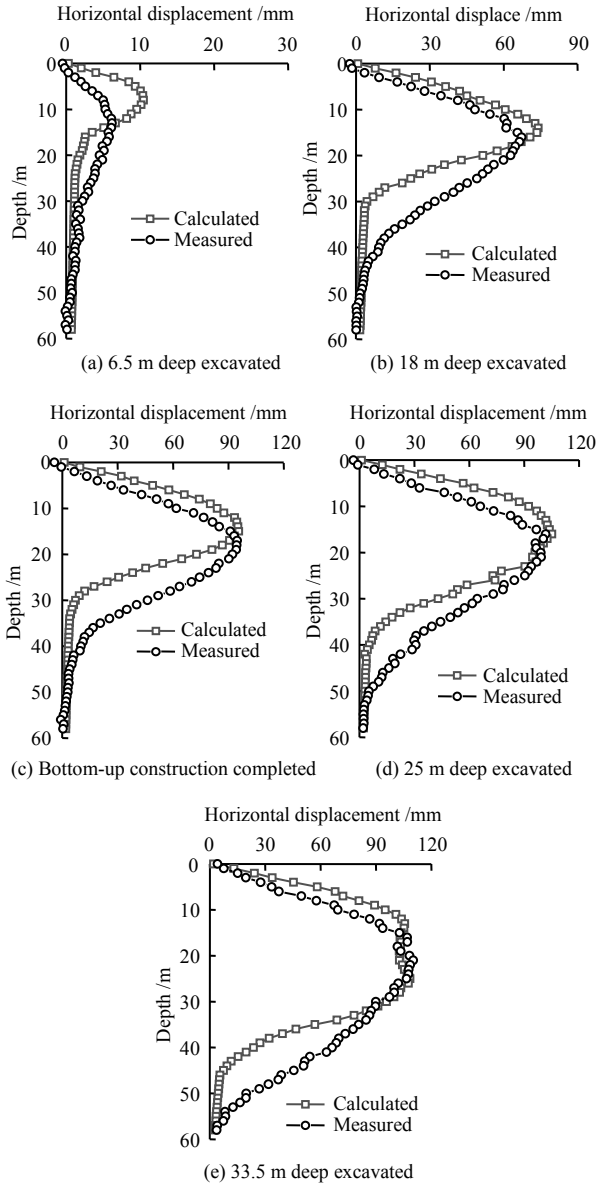

Fig. 22 Comparison of horizontal displacements of diaphragm wall under different conditions

From Fig. 22, when the pit is excavated to 6.5 m deep, there is a big difference between the two, because the excavation depth is small and the spatio-temporal effect is not significant; due to the constraint of the soil, the deformation of the diaphragm wall below the excavation surface calculated by the elastic foundation beam method will be rapidly reduced, so it will be smaller than the measured value. In general, the spatio-temporal effect becomes more and more significant with the increase of excavation depth, and the results calculated by the proposed method will gradually match with the measured values, which verifies the rationality of the proposed method.

6 Conclusions

The finite element analysis of the foundation pit support considering the construction process was carried out based on the excavation project of a subway station foundation pit in the Yangtze River floodplain, and its rationality was verified by comparing with the measured data. The retaining structure deformation calculation method in which the spatio-temporal effects are characterized by the coefficient of corner effect K_{ij} and the equivalent horizontal resistance coefficient K_{h} was proposed, and its accuracy has been verified by engineering examples. The conclusions are as below:

(1) The spatial effect is the greatest at the corners of the foundation pit and decreases gradually towards the mid-span. When the aspect ratio of the pit is large, the spatial effect within a certain range of the span is negligible. The coefficient of corner effect K_{ij} is used to characterize the spatial effect on the horizontal displacement of the diaphragm wall. If the soil layer is homogeneous, the distribution of K_{ij} tends to be the same from the pit corner to the mid-span, below a certain depth of the diaphragm wall, when the pit is excavated deeper.

(2) With the unsupported time and excavation depth increasing, the displacement of the diaphragm wall below the excavation surface varies exponential–linear compositely in a certain period, which corresponds to the variation pattern calculated by the equivalent horizontal resistance coefficient K_{h} that characterizes the temporal effect.

(3) The calculation method for the deformation of the retaining structure of the diaphragm wall considering the spatio-temporal effect has been proposed based on the retaining structure deformation calculated by the method in the *Code*, adopting the equivalent horizontal resistance coefficient K_{h} and the influence coefficient of corner effect K_{ij} to characterize the spatio-temporal effect. The necessity of considering the spatio-temporal effect has been verified by practical engineering. And the results calculated by the proposed method are in good agreement with the measured data when the foundation pit is excavated deeply, which can well reflect the spatio-temporal effect on the deformation of retaining structure.

References

[1] YIN Li-jie, LI Yu-jie, ZHU Yan-peng, et al. Monitoring and numerical simulation of support for foundation pit at Yanyuan road station of Lanzhou metro[J]. Chinese

Journal of Geotechnical Engineering, 2021, 43(Suppl.1): 111–116.

[2] ZHANG Y, YI L, ZHANG L, et al. Causation identification and control measures of deformation by integrated dewatering-excavation process simulation of a t-shaped deep foundation pit[J]. Water, 2022, 14(4): 535.

[3] WAN Xing, GE Ming, HE Zhi-jiang, et al. Characteristics of deformation of retaining wall due to deep excavation in Nanjing[J]. Chinese Journal of Geotechnical Engineering, 2019, 41(Suppl.1): 85–88.

[4] LIU Nian-wu, CHEN Yi-tian, GONG Xiao-nan, et al. Analysis of deformation characteristics of foundation pit of metro station and adjacent buildings induced by deep excavation in soft soil[J]. Rock and Soil Mechanics, 2019, 40(4): 1515–1525, 1576.

[5] QIN Hui-lai, HUANG Jun, LI Qi-zhi, et al. Influencing factors for deformation of deep foundation pits in thick mud stratum[J]. Chinese Journal of Geotechnical Engineering, 2021, 43(Suppl.2): 23–26.

[6] WANG Gui-ping, LIU Guo-bin. Finite element analysis of the deformation of deep excavations considering time-space effect in soft soils[J]. China Civil Engineering Journal, 2009, 42(4): 114–118.

[7] ZHENG Gang. Method and application of deformation control of excavations in soft ground[J]. Chinese Journal of Geotechnical Engineering, 2022, 44(1): 1–36, 201.

[8] CHEN T, SONG J, ZHAI C. Analysis and study of deformation of foundation pit excavation in soft soil considering time-space effect[J]. Geotechnical Engineering Technique, 2019, 33(3):149–153, 187.

[9] GAO Wen-hua, YANG Lin-de, SHEN Pu-sheng. Analysis of influencing factors of time-space effect of internal force and deformation of deep foundation pit retaining structure in soft soil[J]. China Civil Engineering Journal, 2001, 34(5): 90–96.

[10] LIU L L, WU R G, CONGRESS S S, et al. Design optimization of the soil nail wall-retaining pile-anchor cable supporting system in a large-scale deep foundation pit[J]. Acta Geotechnica, 2021, 16(7): 2251–2274.

[11] LIU Jian-hang, LIU Guo-bin, FAN Yi-qun. Theory and practice of space-time effect in soft soil foundation pit engineering (Part 1)[J]. Tunnel and Rail Transit, 1999(3): 7–12, 47.

[12] LIU Jian-hang, LIU Guo-bin, FAN Yi-qun. Theory and practice of space-time effect in soft soil foundation pit engineering (Part 2)[J]. Tunnel and Rail Transit, 1999(4): 10–14.

[13] LIU Yan, LIU Guo-bin, SUN Xiao-ling, et al. Analysis of deformation laws by using the rule of time-space effectin soft soil excavation[J]. Chinese Journal of Geotechnical Engineering, 2006, 28(Suppl.): 1433–1436.

[14] YING Hong-wei, XIE Kang-he, PAN Qiu-yuan, et al. Finite element analysis of excavation time effect of soft clay deep foundation pit[J]. Chinese Journal of Computational Mechanics, 2000(3): 349–354.

[15] HARAHAP S E, OU C Y. Finite element analysis of time-dependent behavior in deepexcavations[J]. Computers and Geotechnics, 2020, 119: 103300.

[16] LI Tao, YANG Yi-wei, JIA Ao-yun, et al. Prediction of three-dimensional surface deformation of long and narrow deep foundation pit under spatial effect[J]. Journal of China University of Mining & Technology, 2020, 49(6): 1101–1110.

[17] ZHANG Kun-yong, ZANG Zhen-jun, LI Wei, et al. Three-dimensional elastoplastic model of soil with consideration of unloading stress path and its experimental verification[J]. Rock and Soil Mechanics, 2019, 40(4): 1313–1323.

[18] LIU W, ZHAO T, ZHOU W, et al. Safety risk factors of metro tunnel construction in China: an integrated study with EFA and SEM[J]. Safety Science, 2018, 105: 98–113.

[19] YU Y L, WU K, CUI S S, et al. Deformation characteristics analysis of supporting structure caused by deep excavation of large-span subway parking lot in deep silt stratum[J]. Indian Geotechnical Journal, 2019, 49(5): 519–530.

[20] OU C Y, CHIOU D C, WU T S. Three-dimensional finite element analysis of deep excavations[J]. Journal of Geotechnical Engineering, 1996, 122(5): 337–345.

[21] WANG Xiao-wei, TONG Hua-wei. Deformation calculation of supporting structure considering deep excavation pit corner[J]. Chinese Journal of Underground Space and Engineering, 2011, 7(3): 479–484.

[22] LIU Guo-bin, HUANG Yuan-xiong, HOU Xue-yuan. Study on the value of horizontal resistance coefficient of equivalent soil considering space-time effect[J]. China Civil Engineering Journal, 2001, 34(3): 97–102.